Supplement of

# An Improved Model of Shade-affected Stream Temperature in Soil & Water Assessment Tool

This supplement provides details of some calculation processes performed in the study. This is divided into five parts:

- S1 Including Water Rights into SWAT Model;
- S2 Shade Factor Calculation;
- S3 Calibrated parameters for flow and stream temperature;
- S4 Shade Factor Temporal Variation; and
- S5 Effects of Riparian Vegetation on the Shade-Factor and Stream Temperature.

## S1 Including Water Rights into SWAT Model

Oregon establishes that water belongs to the public. Irrigation, business, and other water-use activities must obtain a license from the Water Resources Department of Oregon for taking and using water from any source. This law is applied to all types of water sources (rivers, lakes, groundwater). Thus, since the approval of this law, in the DMW like in other areas of Oregon, water-use rights have been given to users, which were considered here for flow modelling (OWRD, 2018).

### S1.1 Stakeholder Water Rights

Statewide water-right spatial data in ArcGIS format was obtained from the Oregon Water Resources Department website (OWRD, n.d.). This information involves metadata of Point-of-Diversion (POD), Places of Use (POU) with water rights. The POU data involves information such as the purpose of water use, land area, the certificate number, priority, the SNP id, among others. The POD data involves information such as the catchment point location, the purpose of water use, the certificate number, source (stream, lake, well), SNP id, allowed period to take water, duty (maximum volume of water allowed to take from the source), maximum rate of water allowed to take from the source, among other data.

After processing water-rights metadata for irrigation purposes (codes: irrigation and supplemental irrigation) for DMW, 785 POUs and 937 PODs were found. The difference between the number of PODs and POUs was because in some cases, one POU was irrigated by two or three PODs, and in very few cases one POD irrigated more than one POU (Fig. S1). PODs and POUs were matched by using the SNAP-ID. Thus, for DMW, 785 pairs of POD-POU were obtained (Fig. S2).

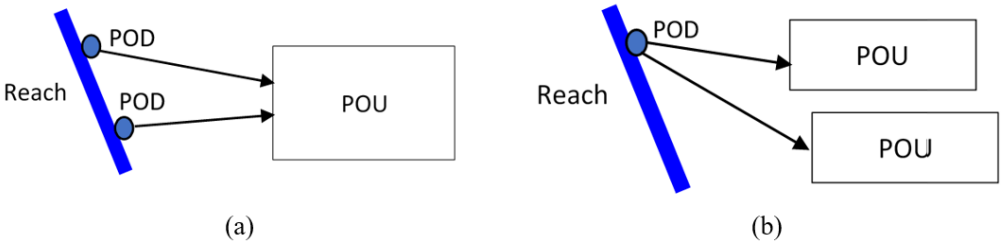


**Figure S1. (a) one POU irrigated by two PODs. (b) one POD irrigating two POUs**

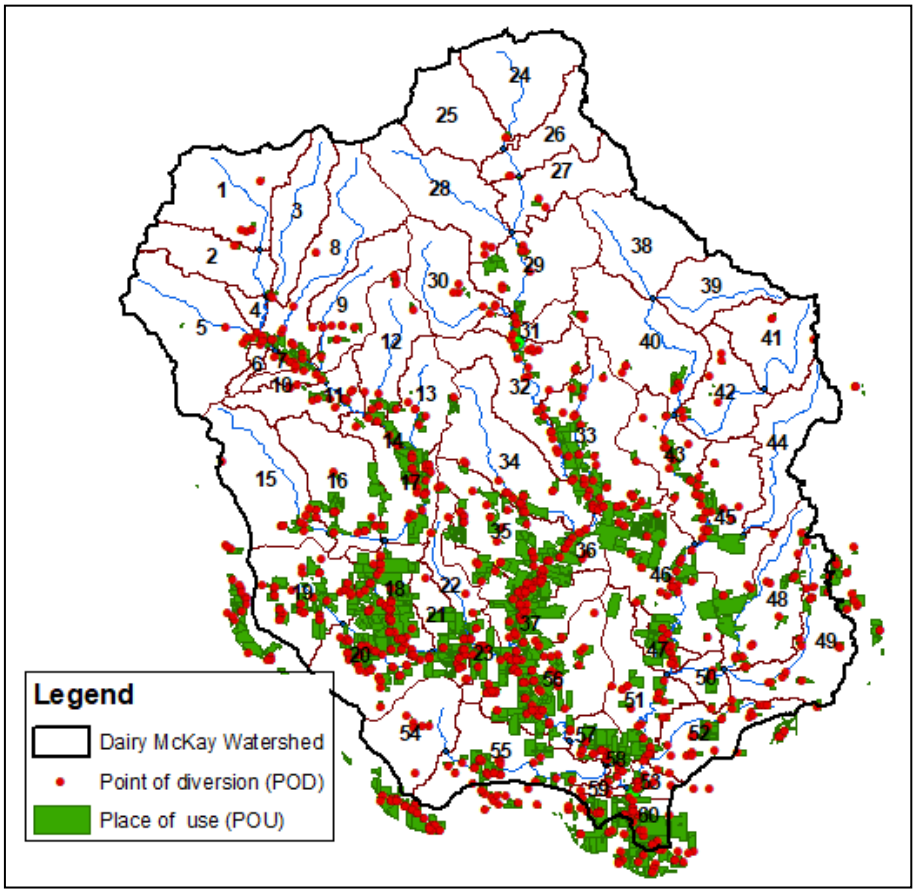


**Figure S2. Distribution of Points of diversion (PODs) and Places of use (POUs) with water rights within the Dairy McKay watershed.**

### S1.1.1 Period of Operation according to Water Rights

According to water rights, 75.2% of PODs are allowed to uptake water from their source over the year, by 21.7% of PODs are allowed to uptake water over eight months (from March to October), and only 3.1% of PODs are allowed to uptake water for less than eight months. For modelling purposes, this research considered only two periods for uptake of water (twelve and eight months).

### S1.1.1 Assignation of Maximum Water Volume to HRUs.

Edges of POUs do not necessarily matched with edges of SWAT Hydrologic Response Unit (HRU), so that, to transfer the information of the maximum water volumes assigned to the POUs to the HRUs, a weighting relationship of proportion of areas was employed. Thus, the maximum volume of water of an HRU was equal to the sum of the maximum volume of water of each POU multiplied by its percentage of the area lying over the HRU (Eq. S1, Fig. S3).

$$V_{HRU_j} = \sum_{i=1}^{n} \frac{w_{ij} \cdot V_{POU_{ij}}}{100} \quad \text{(S1)}$$

Where $V_{HRU_j}$ is the maximum volume of uptaking water for $HRU_j$, $V_{POU_{ij}}$ is the maximum volume of uptaking water of the $POU_i$, $w_{ij}$ is the rate of the $POU_i$ lying over the $HRU_j$, $n$ is the number of POUs that have common areas with the $HRU_j$. Therefore, the sum $(\sum_{i=1}^{n} w_{ij})$ does not necessarily is equal to 1, but the sum $\sum_{i=1}^{n} w_i$ must be equal to 1.

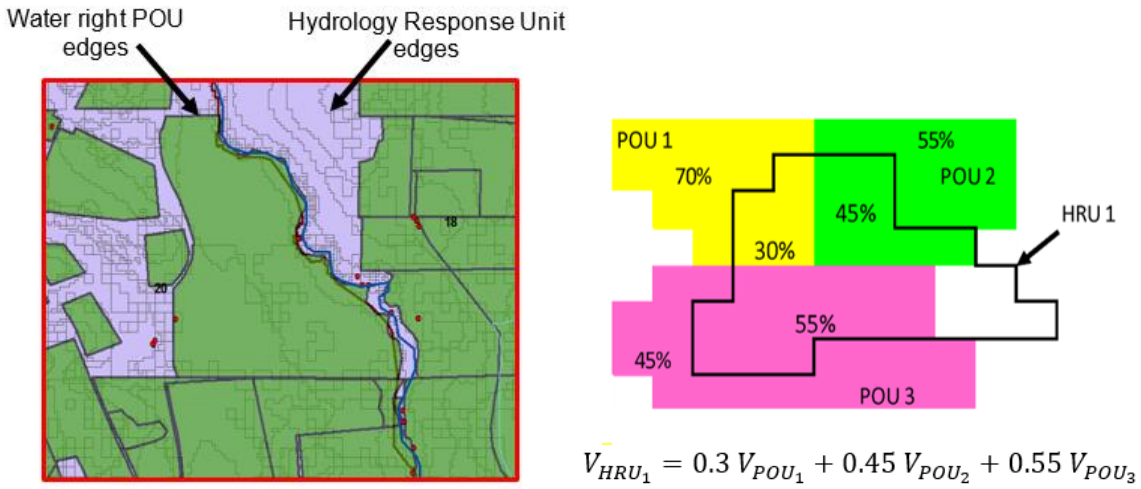


**Figure S3. Assignation of maximum water volume to Hydrological Response Units (SWAT units)**

### S1.2 Including Instream Water Rights (Instream Minimum Flow) into SWAT model

Instream flows in Oregon are protected by the 30th Anniversary of Oregon's Instream Water Right Act. The purpose of this amount of water is to support aquatic life and minimize pollution. According to this law, if a river carries a flow less than or equal to the instream flow water right, no one can withdraw water from the river unless they have a water right prior to the water right established for that stream.

For DMW, six water rights of instream flows were found. These water rights establish control of minimum flows in four sites (McKay Creek measured at or near River mile 15.5 (IWR-1), Denny Creek and its tributaries above its mouth measured at or near the mouth (IWR-2), Plenty-water Creek and its tributaries above its mouth measured at or near the mouth (IWR-3), and East Fork Dairy Creek and its tributaries above river mile 13 measured at or near river mile 13 (IWR-4)) and along two rivers (The West Fork of Dairy Creek and its tributaries at the Highway 47 crossing at banks, and maintained to the mouth (IWR-5), and Dairy Creek from headwaters to the mouth at river mile 0 (IWR-6)). Most of these water rights do not consider a constant flow during the year as shown in Fig. S4. These water rights were also considered here in the SWAT flow modeling as the minimum instream flow for irrigation diversion.

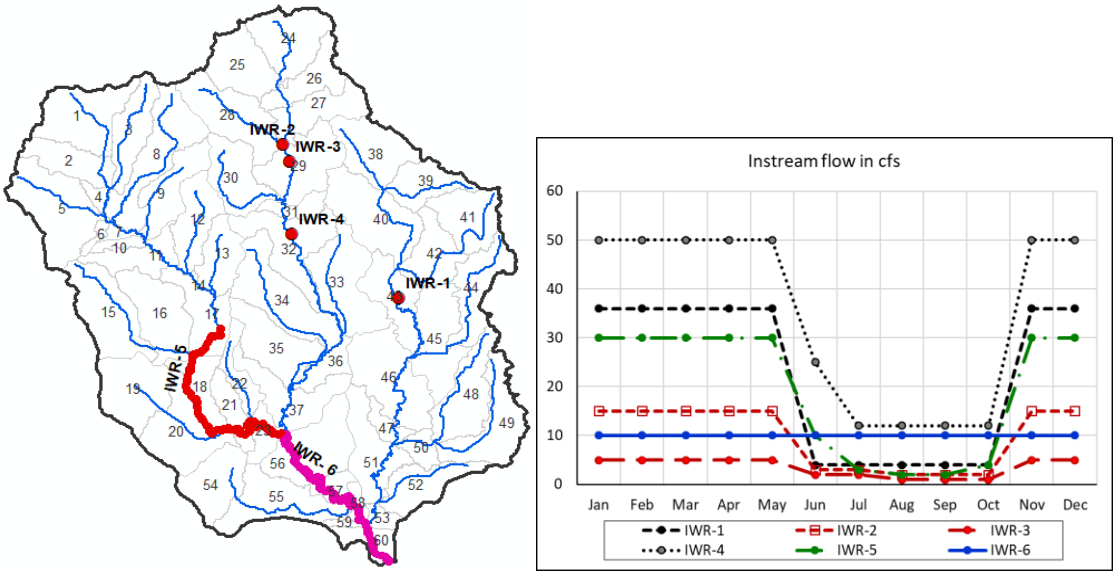


**Figure S4. DMW streams with water rights establishing the minimum in-stream flow**

70

## S2 Shade Factor Calculation

The shade factor was computed as the rate of solar radiation blocked by the topography and riparian vegetation divided by the potential solar radiation that would reach the stream surface. The blocked solar radiation was determined by the shaded area in the stream generated by the topography and vegetation of the stream banks.

The blocked solar radiation was determined for time intervals of 0.01 hours and was accumulated during the day (from sunrise to sunset) to determine a more accurate SF for the whole day and for all days in the year. This calculation process was developed in the Python environment and then input into the SWAT hydrological model (https://github.com/noayarae/SF_model.git). Side banks have been distinguished throughout the calculation process to identify the contribution of each bank in the SF increase and then in the stream temperature decrease. Table S1 shows the steps followed to calculate the SF. These steps were repeated for 365 days and for each stream within the DMW. Below are the equations used in the calculation of the shade factor.

**Table S1. Steps to calculate the shade factor for each day (pseudocode)**

```
Calculate latitude, stream azimuth, and stream length
Calculate the topographic angle from DEM
Get stream width from the SWAT model
Get height tree for each stream bank from the Landfire database
Start loop through the 24 hr. (Δt = 0.01 hr.)
    Calculate solar angle and solar azimuth for each time step (Eq. S2, Eq. S5)
    Calculate the solar radiation for each time step (Eq. S6)
    If solar angle > 0 & Potential solar radiation > 0
        Calculate the length of the shadow parallel to the solar azimuth (Eq. S9)
        Calculate the length of the shadow normal to the stream (Eq. S10)
        Calculate the shadow over the stream
        If top_angle > solar angle: (The shade is caused by topography)
            The shade corresponds to the topography
        If top_angle < sola angle: (The shade is caused by riparian vegetation)
            The shade corresponds to the riparian vegetation
            Identify the riparian bank causing the shadow
                If sin (solar_angle – strm_azimuth) > 0 → Right bank
                If sin (solar_angle – strm_azimuth) < 0 → Left bank
    Calculate the accumulated solar radiation no reaching the stream during the day
    Calculate the potential solar radiation that might reach the stream during the day
Calculate the daily shade factor (SF_i = SR_daily / SR_potential) (Eq. S11)
```

### S2.1 Solar Angle and Solar Azimuth

The solar angle is measured between the observer's horizon and the sun. It is a function of the stream latitude, declination of the sun, and the time of the day (Eq. S2-S4).

$$\alpha = \sin^{-1}(\sin\phi.\sin\delta + \cos\phi.\cos\delta.\cos\tau) \quad \text{(S2)}$$

$$\delta = 23.45 \left(\frac{2\pi}{360}\right) cos\left(\frac{2\pi\,(172-JD)}{365}\right) \quad \text{(S3)}$$

$$\tau = \left(180 - long - t_m - (360\ hr/24)\right)(2\pi/360) \quad \text{(S4)}$$

Where: $\alpha$ is the solar altitude (solar angle), $\phi$ is the stream latitude, $\delta$ is the declination of the sun, $\tau$ is the local hour angle of the sun, $JD$ is the Julian day (1-365), $long$ is the stream longitude, $t_m$ is the local time zone meridian (degrees), and $hr$ is the hour of the day. These equations are explained in depth by Boyd (Boyd 2003).

The solar azimuth is the angle formed by north and the horizontal projection of the sun (on the observer's horizon) measured clockwise (Eq. S5).

$$Sun_{az} = \cos^{-1}\left(\frac{\sin\delta - \sin\alpha\,.\,\sin\phi}{\cos\alpha\,.\,\cos\phi}\right) \quad \text{(S5)}$$

Stream azimuths were measured from the north to the stream center line in the flow direction. These values were obtained in the GIS environment for each stream of each sub-basin.

### S2.2 Sub Daily Solar Radiation

Solar radiation for sub-daily time scales was obtained using the Kaplanis approach (Kaplanis, 2006; Khatib & Elmenreich, 2015). This approach proposes solar radiation at any time as a cosine function limited by the sunrise and sunset and conditioned to the day (Eq. S6).

$$h_{ij} = a.n_j + b.n_j\ cos(\frac{2\pi\,t_{ss}}{24}) \quad \text{(S6)}$$

Where $h_{ij}$ is the solar radiation at any time within the day, $t_i$ is the time in hours, $n_j$ is the Julian day, and $a$ and $b$ are coefficients determined for any site and any day. These coefficients are determined by solving the Eq. (S6) for the following boundary conditions: the integration of the above equation over $h$, from sunrise ($t_{sr}$) to sunset ($t_{ss}$) is equal to the measured daily solar radiation, and the solar radiation when $h$ equals $t_{ss}$ is zero (For $t_i = t_{ss}$, $h_{ij} = 0$) (Kaplanis, 2006) (Eq. S7-S8).

$$H_j = \int_{t_{sr}}^{t_{ss}} h_{ij}\ dt \quad \text{(S7)}$$

$$a.n_j + b.n_j.\cos(2\pi\,t_{ss}/24) = 0 \quad \text{(S8)}$$

### S2.3 Shadow over the Stream

The length of the shadow (Laz) (either by riparian or the topography) parallel to the solar azimuth and length of the shadow normal to the streamflow are obtained by geometry (Fig. S5) (Eq. S9-S10).

$$Laz = \frac{h\_tree}{tan(\alpha)} \quad \text{(S9)}$$

$$L_n = L_{az}\,.sin(sun_{az} - strm_{az}) \quad \text{(S10)}$$

Where $h\_tree$ is the tree height in riparian vegetation, $\alpha$ is the solar angle, $sun_{az}$ is the solar azimuth, and $strm_{az}$ is the stream azimuth.

The normal shadow was then multiplied by the stream length. Thus, three shading scenarios on the stream can be observed: no shadow over the stream, partial shadow over the stream, and full shadow over the stream. In this calculation, the shade factor corresponding to the topography, left bank and right bank (defined in the direction of flow) has been identified and then calculated separately to determine the contribution of each barrier in the stream SF.

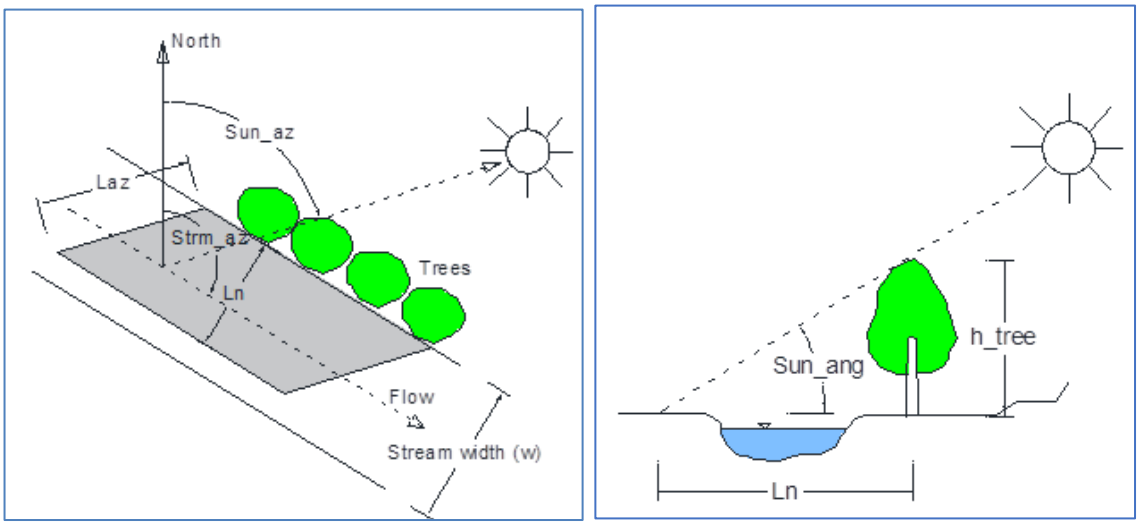


.(a) (b)

**Figure S5. Diagram showing the variables to calculate the length of the shadow parallel to the azimuth (Laz) and perpendicular to the streamline (Ln). (a) perspective and (b) side view.**

Finally, the shade factor for each day and each sub-basin was obtained by dividing the accumulated amount of blocked solar radiation by the potential solar radiation representing the solar heat flux (both diffuse and direct beam) that would reach the stream surface without barriers (S11).

$$SF_{ijk} = \frac{\sum_{k=t_{sr}}^{t_{ss}} Shade_{ijk} \cdot h_{ijk}}{L_j \cdot W_j \, H_{ijk}} \quad \text{(S11)}$$

Where $i$ indicates the number of sub-basin (from 1 to 60 for DMW), $j$ is the day in the year (from 1 to 365), $k$ is the time in the day, $Shade_{ijk}$ is the shade of the barrier on stream, $h_{ijk}$ is the solar radiation at the time $k$, $L_j$ is the stream length, $W_j$ is the surface water width determined by the SWAT model, $H_{ijk}$ is the registered daily solar radiation.

## S3 Calibrated Parameters

### S3.1 Calibrated parameters for flow

After considering several parameters in the flow calibration process, seventeen were selected which are shown in Table S2.

**Table S2. Flow Calibration Parameters.**

| ID | Parameter | Name | Value | |
|---|---|---|---|---|
| | | | SB #31 | SB #59 |
| 001 | ALPHA_BF.gw | Baseflow recession constant | 0.92 | 0.65 |
| 002 | CH_N2.rte | Manning's "n" value for the main channel | 0.029 | 0.072 |
| 003 | CN2.mgt | SCS runoff curve number factor | x 0.85 | x 0.75 |
| 004 | DDRAIN.mgt | Depth to subsurface drain (mm) | 993.5 | 993.5 |
| 005 | EPCO.hru | Plant uptake compensation factor | 0.34 | 0.33 |
| 006 | ESCO.hru | Soil evaporation compensation coefficient | 0.34 | 0.50 |
| 007 | GDRAIN.mgt | Drain tile lag time (hrs) | 34.5 | 34.5 |
| 008 | GW_DELAY.gw | Groundwater delay (days) | 303.48 | 11.69 |
| 009 | GW_REVAP.gw | Groundwater "revap" coefficient | 0.19 | 0.17 |
| 010 | GWQMN.gw | Threshold depth of water in the shallow aquifer required for return flow to occur (mm $H_2O$) | 4978 | 2025 |
| 011 | HRU_SLP.hru | Average slope steepness (m/m) | x 0.88 | x 1.0 |
| 012 | LAT_TTIME.hru | Lateral flow travel time (days) | 10.6 | 10.3 |
| 013 | OV_N.hru | Manning's "n" value for overland flow | 0.025 | 0.052 |
| 014 | RCHRG_DP.gw | Deep aquifer percolation fraction | 0.19 | 0.06 |
| 015 | REVAPMN.gw | Threshold depth of water in the shallow aquifer for "revap" to occur (mm) | 418.3 | 305.5 |
| 016 | SOL_K.sol | Saturated hydraulic conductivity (mm/hr) | 56.0 | 52.2 |
| 017 | TDRAIN.mgt | Time to drain soil to field capacity (hrs) | 18.0 | 18.0 |

### S3.2 Calibrated parameters for stream temperature

**Table S3. Stream Temperature Calibration Parameters for the Modified Ficklin et al. Model**

| Calibration site | $\lambda$ | $T_{air}$-lag (days) | $C_1$ | $C_2$ |
|---|---|---|---|---|
| SB #31 | 0.88 | 5 | 0.67 | 1.16 |
| SB #59 | 1.06 | 6 | 0.74 | 1.17 |

## S4 Shade Factor Temporal Variation

### S4.1 Shade Factor Variation over the Day

Fig. S6 shows the potential solar radiation and the amount of blocked solar radiation by the topography and riparian vegetation for three streams (stream #16, #29, and #39) with different stream azimuths (97.7°, 179.5°, and 269.0°, respectively) and for a typical summer (July 19) and winter (Dec 31) day.

**Summer day** **Winter day**

Stream #16 (Azimuth = 97.7°)

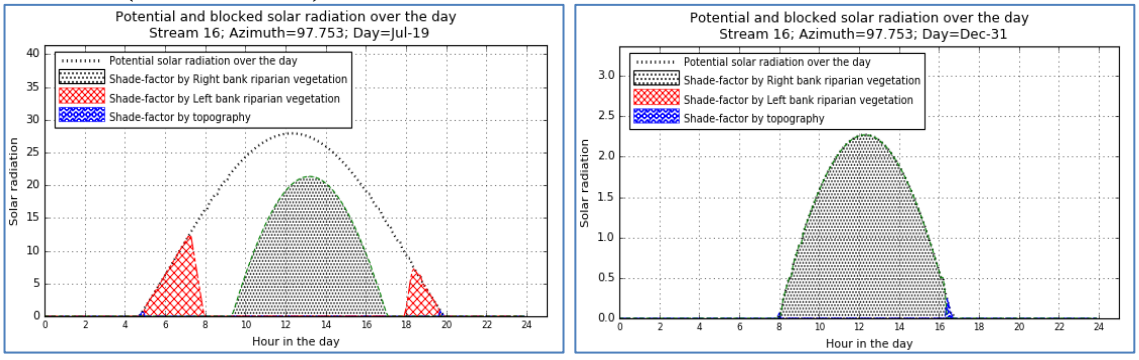


Stream #29 (Azimuth = 179.5°)

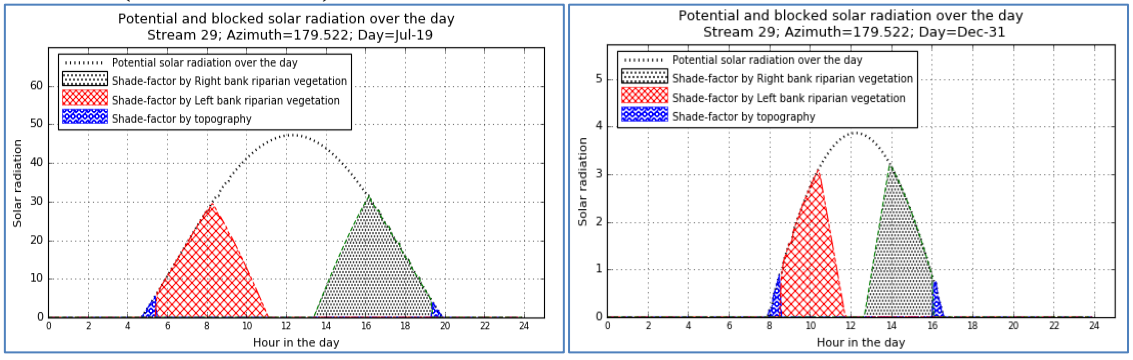


Stream #39 (Azimuth = 269.0°)

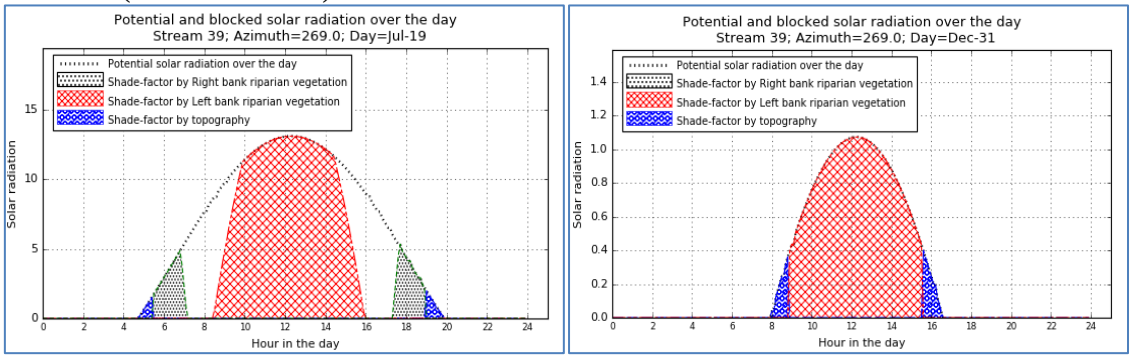

**Figure S6. Potential solar radiation and blocked solar radiation identifying the blocking barrier for three streams with different azimuths and for a typical summer and winter day (Jul-19, Dec-31).**

## S4.2 Shade Factor Variation over the Year

Fig. S7 shows the variation of the shade factor for three streams with varied stream azimuths during the year. For example, in stream #16 (Azimuth = 97.7°) and stream #39 (Azimuth = 269.0°), the northern bank contribution is much lower compared to the southern bank contribution over the year, while for stream #29 both banks contribute in similar amounts to the shade factor.

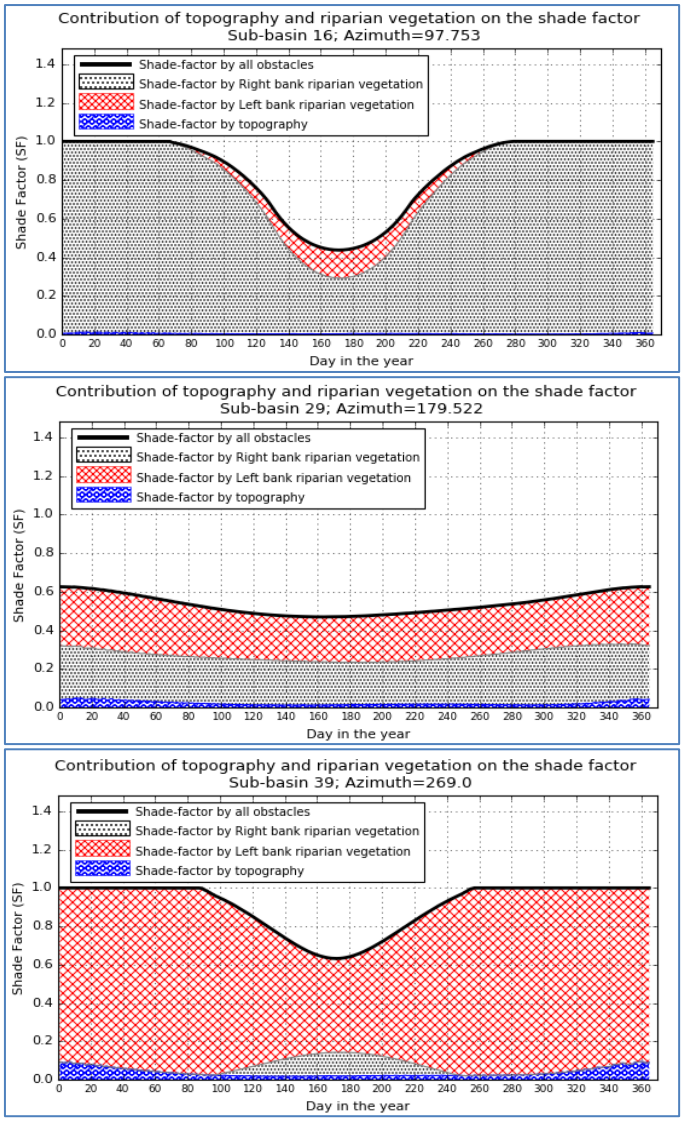


**Figure S7. Shade factor variation over the year for three DMW streams with different azimuths.**

## S5 Effects of Riparian Vegetation on the Shade-Factor and Stream Temperature

Fig. S8 shows the contribution of each bank blocking the solar radiation in scenarios 1 (current riparian vegetation), scenario 2 (full riparian vegetation), and scenario 3 (efficient riparian vegetation) for stream #16 (Azimuth = 97.75°), #29 (Azimuth = 179.5°), and #39 (Azimuth = 269.0°), which have noticeable differences in azimuth, for a summer day (Jul. 19). In streams oriented from W-E and E-W as stream #16 and #39 respectively, the contribution of the northern side riparian vegetation is much less than the southern side. This minor contribution is only shown in the early morning and late afternoon. Scenario 3 practically resembles scenario 2, despite the fact that scenario 3, for streams-oriented E-W and W-E, does not consider the implementation of the northern side vegetation.

Fig. S9 shows the contribution of each bank on the shade factor for stream #16 (Azimuth = 97.75°), stream #29 (Azimuth = 179.5°), and stream #39 (Azimuth = 269.0°) during the year. Here one can also see that in streams oriented from W-E and E-W (stream #16 and #36), the contribution of the northern side riparian vegetation is much less than the southern side. This minor contribution is only shown in summer. Scenario 3 practically resembles scenario 2, despite the fact that scenario 3, for streams oriented from E-W and W-E, does not consider the implementation of the northern side vegetation.

Fig. S10 shows the percentage of contribution of the topography and riparian vegetation in increasing the shade factor as a function of the stream azimuth. The stream azimuth and banks are considered in reference to the flow direction. To illustrate, in sub-basin #55 (azimuth = 94.1°), the right-bank contribution is 94.7% while the left-bank and topography contribution is only 5.2% and 0.1%, respectively.

Fig. S11 shows the percentage of contribution of the riparian vegetation on the stream temperature reduction as a function of the stream azimuth. The stream azimuth and banks are considered in reference to the flow direction. For instance, in sub-basin #55 (azimuth < 180°), the right-bank contribution is 89.8% while the left-bank contribution is only 10.2%.

Fig. S12 shows the relationship between the reduction of the number of days in the year (a) and in summer (b) with 7dAM stream temperatures exceeding 18 °C, and the shade factor increase for Scenarios 2 and 3. The Fig. shows a positive relationship between these two variables, indicating that as the shade factor increases, the reduction of number of days with 7dAM exceeding 18 °C also increases.

Fig. S13 shows two hydrographs. The first corresponding to the reduction of the average temperature (Fig. S13a) and the second to the reduction of the number of days that exceed 18 °C (Fig. S13b) for scenarios of full and efficient restoration. In both cases, it can be visually observed that both restoration scenarios reach similar reductions.

| | Scenario 1 | Scenario 2 | Scenario 3 |
|---|---|---|---|
| Stream #16 (Azimuth = 97.7°) | 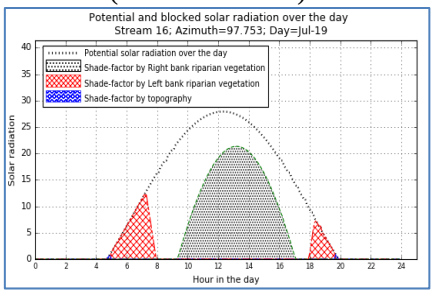 | 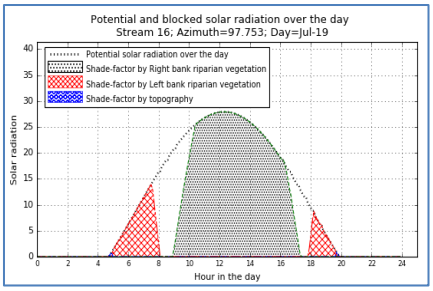 | 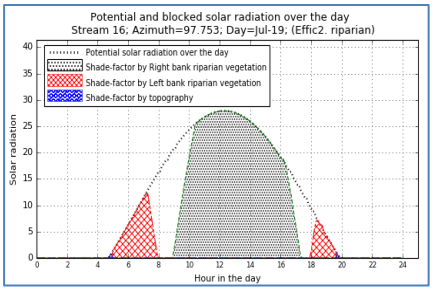 |
| Stream #29 (Azimuth = 179.5°) | 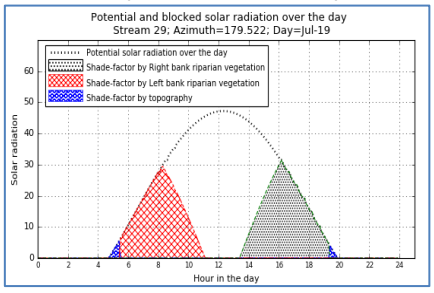 | 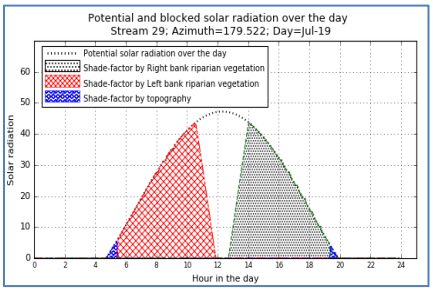 | 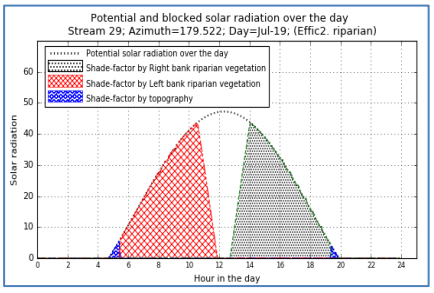 |
| Stream #39 (Azimuth = 269.0°) | 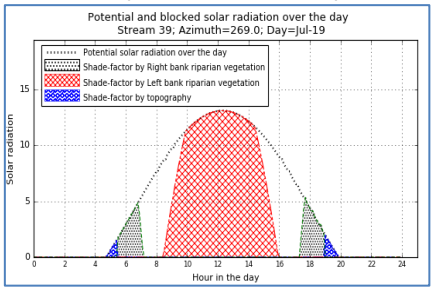 | 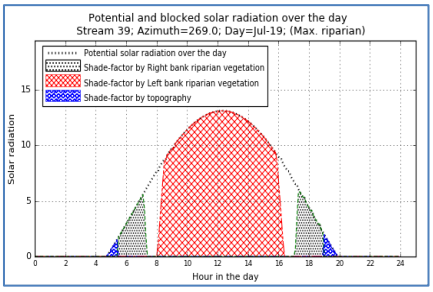 | 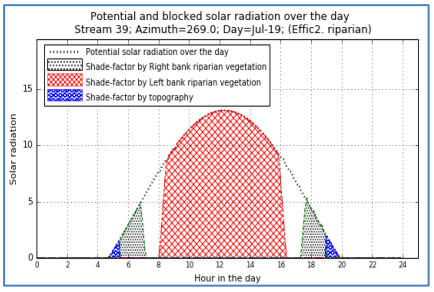 |



**Figure S8. Potential solar radiation and blocked solar radiation identifying the blocking barrier for three streams with different azimuths, for a typical summer day (Jul-19), and for scenarios 1, 2, and 3.**

| | Scenario 1 | Scenario 2 | Scenario 3 |
|---|---|---|---|
| Stream #16 (Azimuth = 97.7°) | 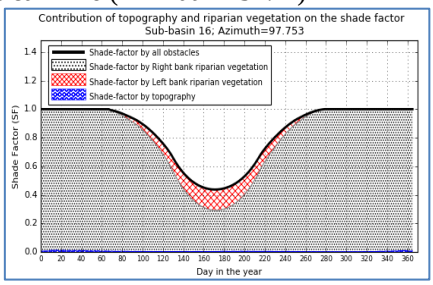 | 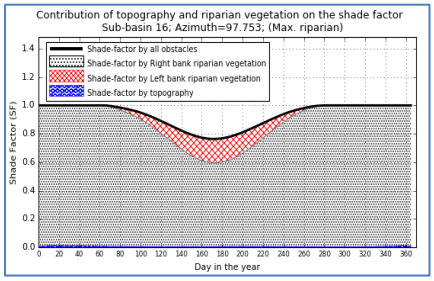 | 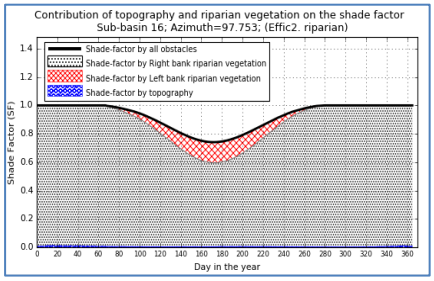 |
| Stream #29 (Azimuth = 179.5°) | 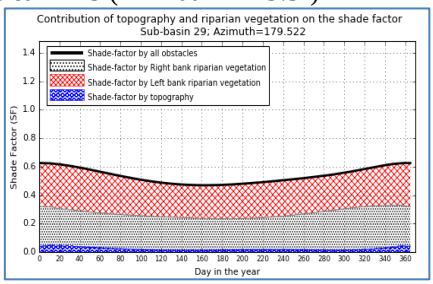 | 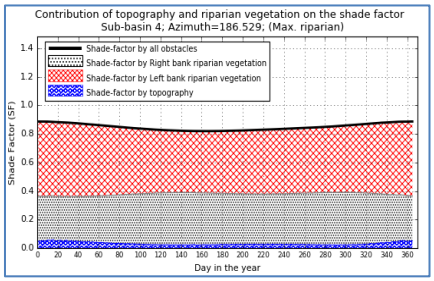 | 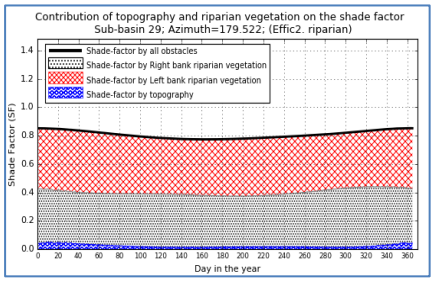 |
| Stream #39 (Azimuth = 269.0°) | 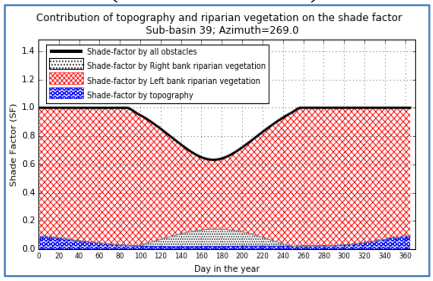 | 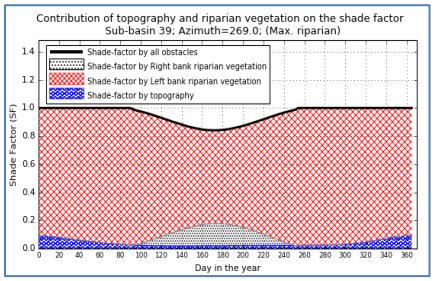 | 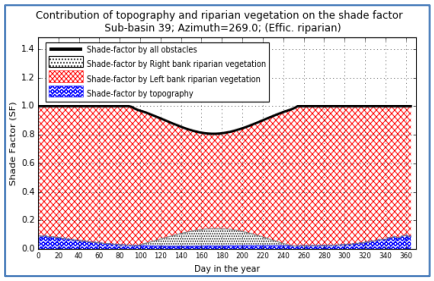 |

**Figure S9. Shade factor variation over the year for three DMW streams with different azimuths and for scenarios 1, 2, and 3.**

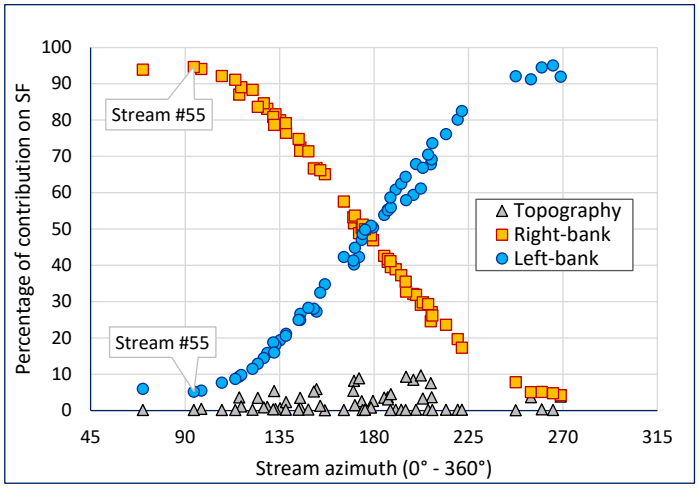


**Figure S10. Contribution of each bank on SF versus stream orientation (azimuth). The right and left bank were defined in the flow direction.**

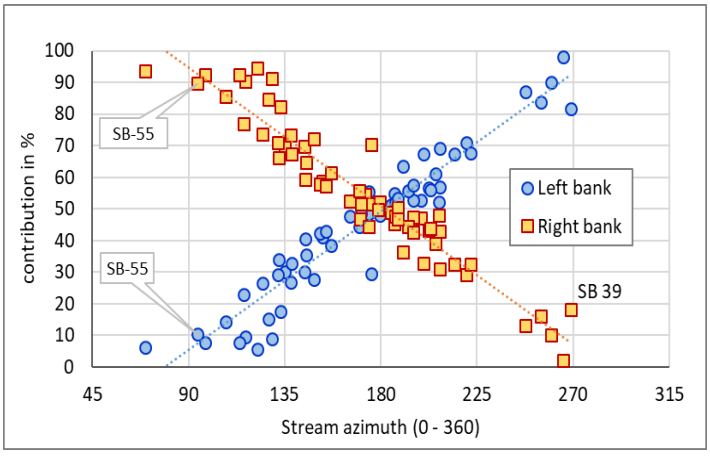


**Figure S11. Percentage of contribution of each bank riparian vegetation on the stream temperature reduction versus the stream orientation (azimuth). The right and left bank were defined in the flow direction**

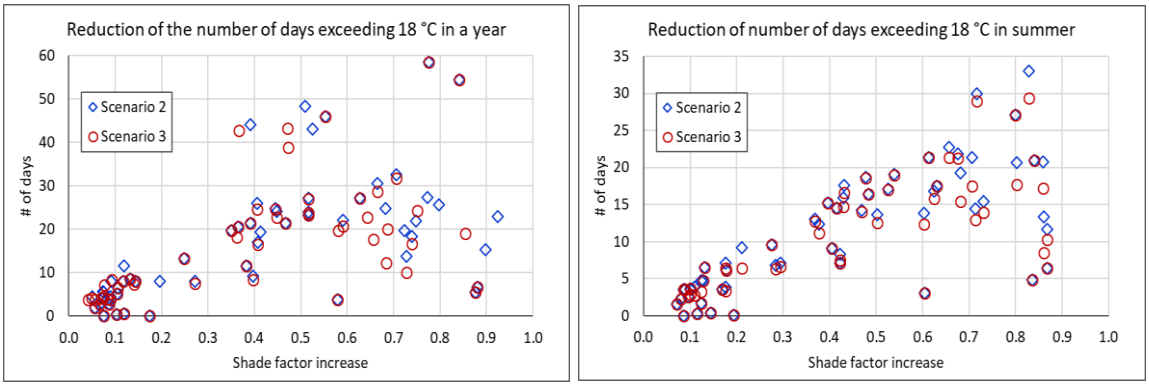


.(a) (b)

**Figure S12. Relationship between the reduction of the number of days in the year (a) and in summer (b) with 7dAM stream temperatures exceeding 18 °C, and the shade factor increase for Scenarios 2 and 3.**

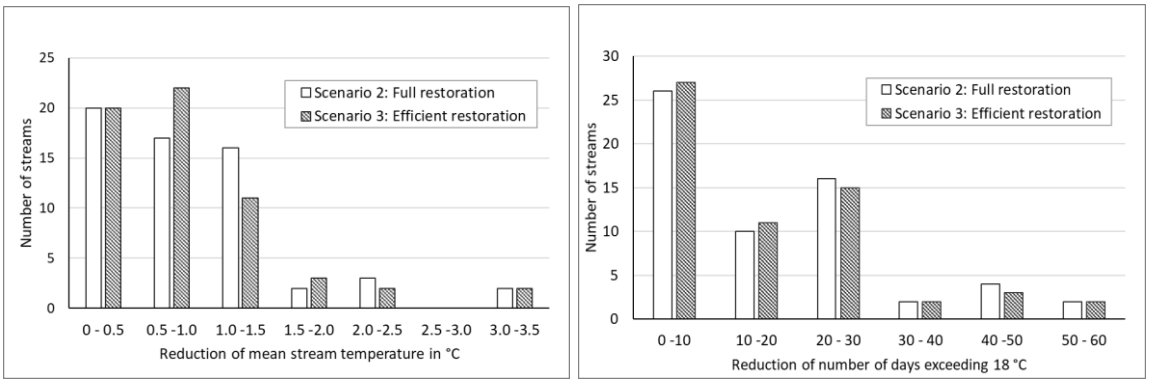


.(a) (b)

**Figure S13. (a) Histogram of stream temperature reductions in the 60 DMW streams for full and efficient riparian restoration. (b) Histogram of reduction of the number of days that exceed 18 °C in the 60 DMW streams for cases of full and efficient riparian restoration.**

**References**


Kaplanis, S. N.: New methodologies to estimate the hourly global solar radiation; Comparisons with existing models. *Renewable Energy*, *31*(6), 781–790. https://doi.org/10.1016/j.renene.2005.04.011, 2006.

Khatib, T., & Elmenreich, W.: A model for hourly solar radiation data generation from daily solar radiation data using a generalized regression artificial neural network. *International Journal of Photoenergy*, *2015*. https://doi.org/10.1155/2015/968024, 2015.

OWRD.: *Water Rights*. Oregon Water Resources Department. Retrieved December 7, 2021, from https://www.oregon.gov/owrd/access_Data/Pages/Maps.aspx, n.d.

OWRD.: *Water Rights in Oregon - An Introduction to Oregon's Water Laws* (Issue September 2009). https://www.oregon.gov/OWRD/WRDPublications1/aquabook.pdf, 2018.